Electronic Supplementary Material (ESI) for RSC Advances.


# Preparation and in vivo imaging of NIR-emissive Carbonized Polymer Dots derived from biomass olive leaves with a quantum yield of 71.4%

*Zhiqiang Zhao[a,#], Qin Luo[b,#], Shengjing Chu[c,#], Qinghui Wen[b], Zhiqiang Yu[b], Jijun Xu[d*], Weibing Xu[c*], Muhua Yi[e*]*

[a.] *Department of Basic Medical Sciences, Medical College of Taizhou University, Taizhou 318000, Zhejiang, China.*

[b.] *Department of Laboratory Medicine, Dongguan Institute of Clinical Cancer Research, Affiliated Dongguan Hospital, Southern Medical University, Dongguan 523018, China.*

[c.] *College of Life Science, Gansu Agricultural University, Lanzhou 730000, China.*

[d.] *Gansu Institute for Drug Control, Lanzhou 730070, China.*

[e.] *Department of Pathology, Affiliated Dongguan Hospital, Southern Medical University, Dongguan 523018, China.*

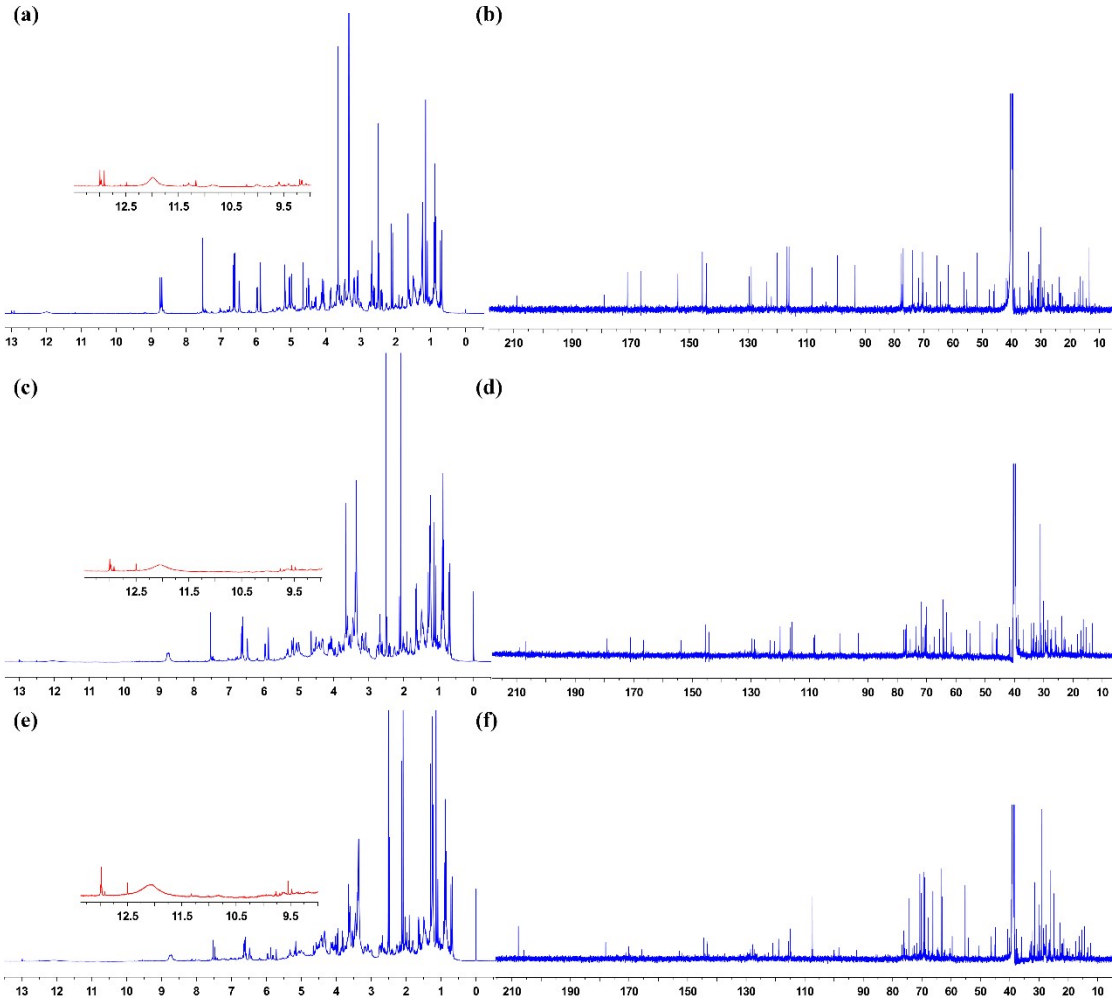


**Fig. S1** (a) $^{1}H$ and $^{13}C$ spectrum of the RCQDs-120 (a, b), RCPDs-150 (c, d) and RCPDs-180 (e, f).

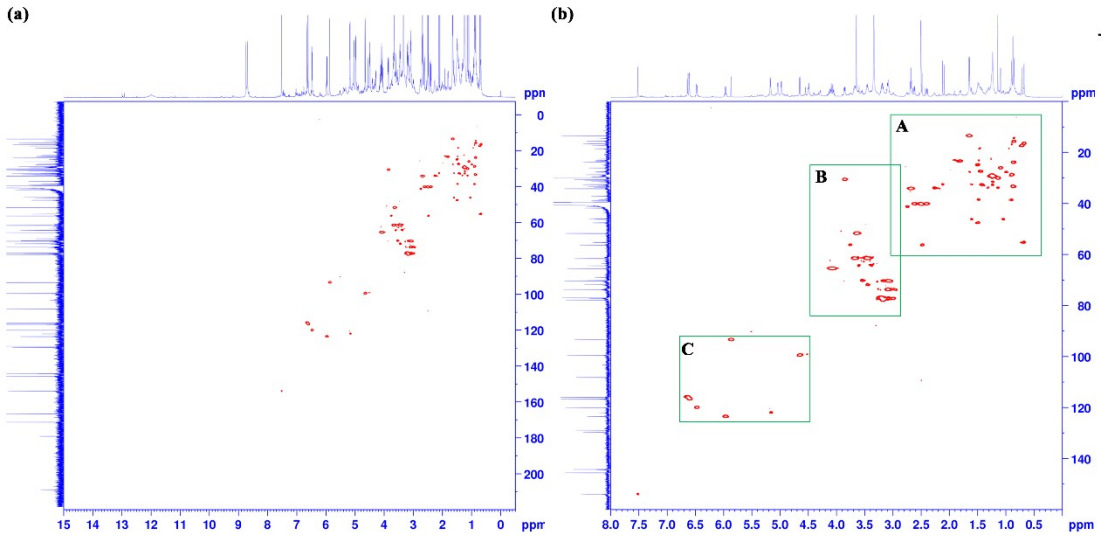


**Fig. S2** HQSC full (a) and partially enlarged (b) spectrum of the RCQDs - 120.


**Fig. S3** the SAED patterns of RCPDs-120 (a), RCPDs-150 (b) and RCPDs-180 (c).

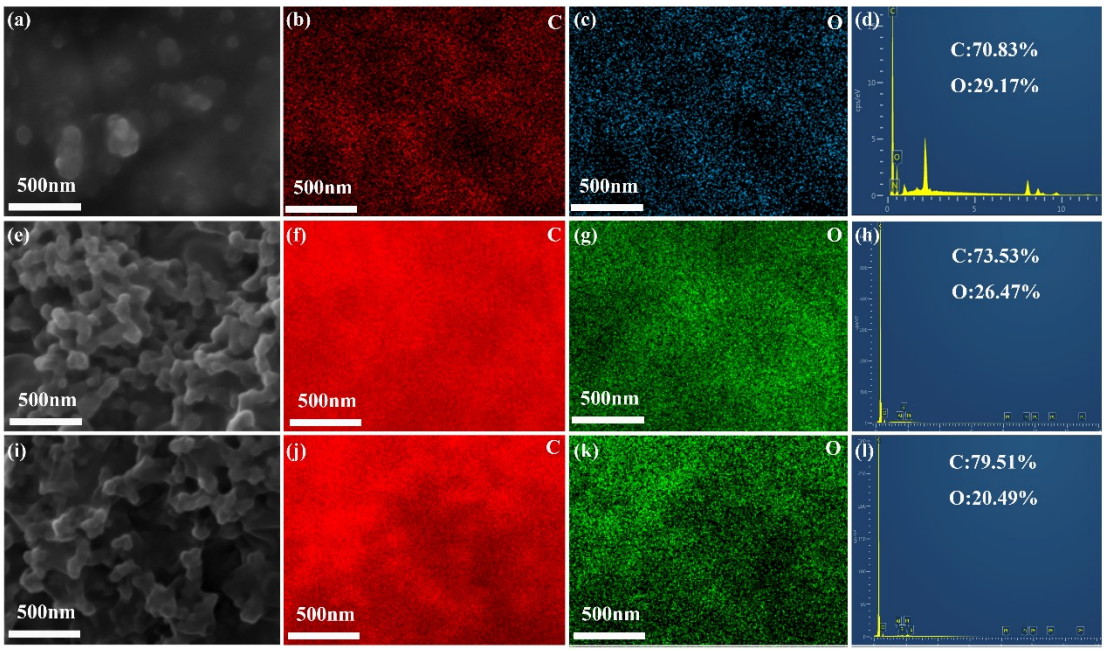


**Fig. S4** The corresponding EDS curve and elements mapping of RCPDs-120 (a-d), RCPDs-150 (e-h) and RCPDs-180 (i-l).

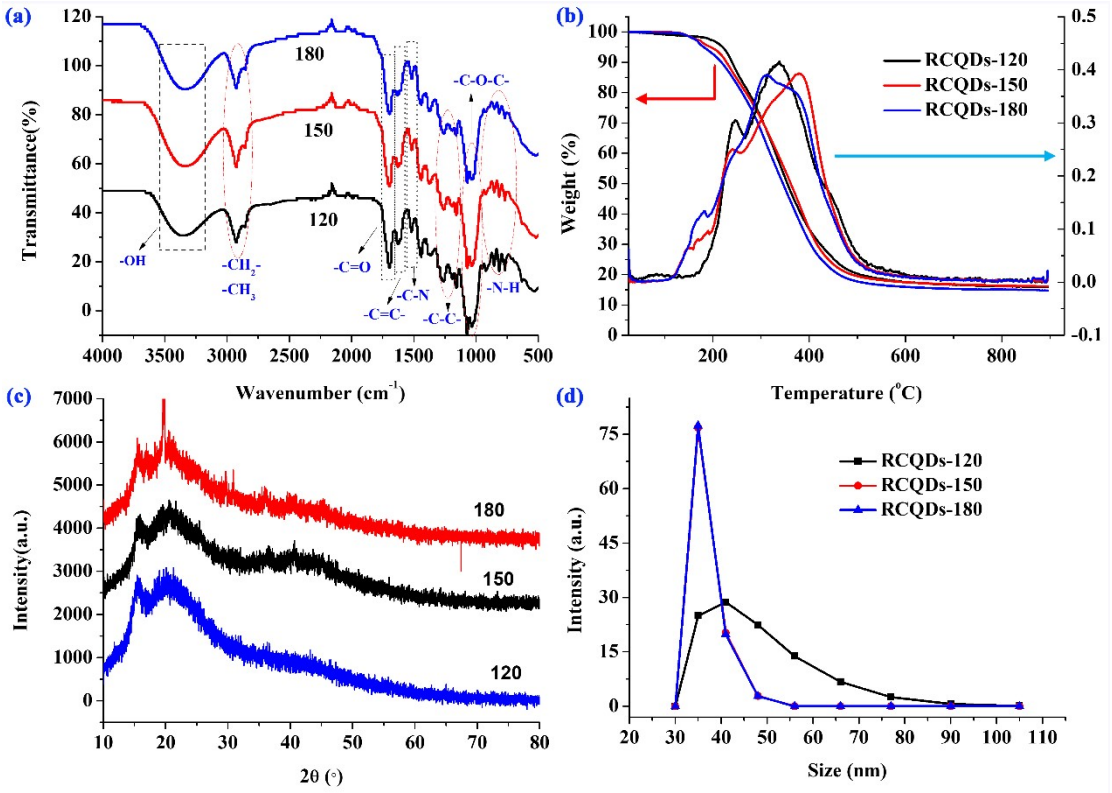


**Fig. S5** The corresponding FTIR spectra (a), TGA and DTG curve (b), XRD patterns (c) and size curves (d) of RCPDs-120, RCPDs-150 and RCPDs-180.

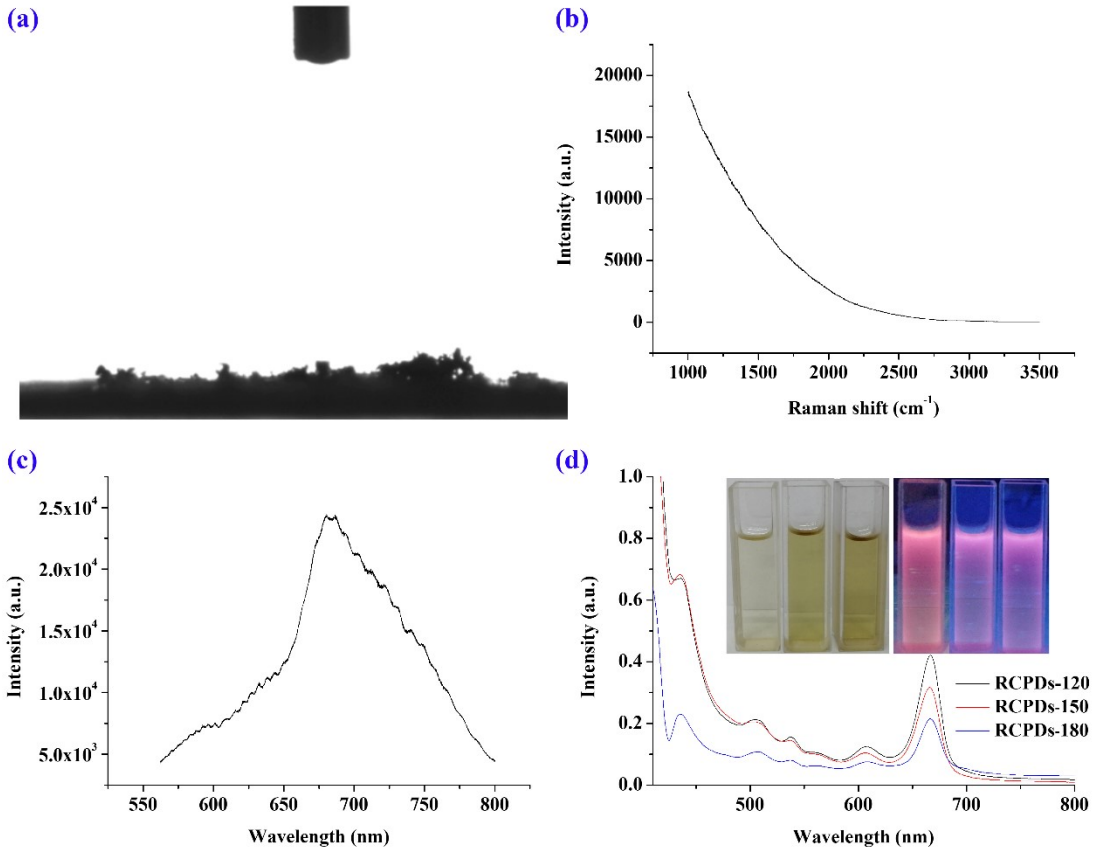


**Fig. S6** The corresponding contact angle image (a), Raman spectrum (b), PL spectrum (c) of RCPDs-120 and UV-Vis curves (d) of RCPDs-120, RCPDs-150 and RCPDs-180.

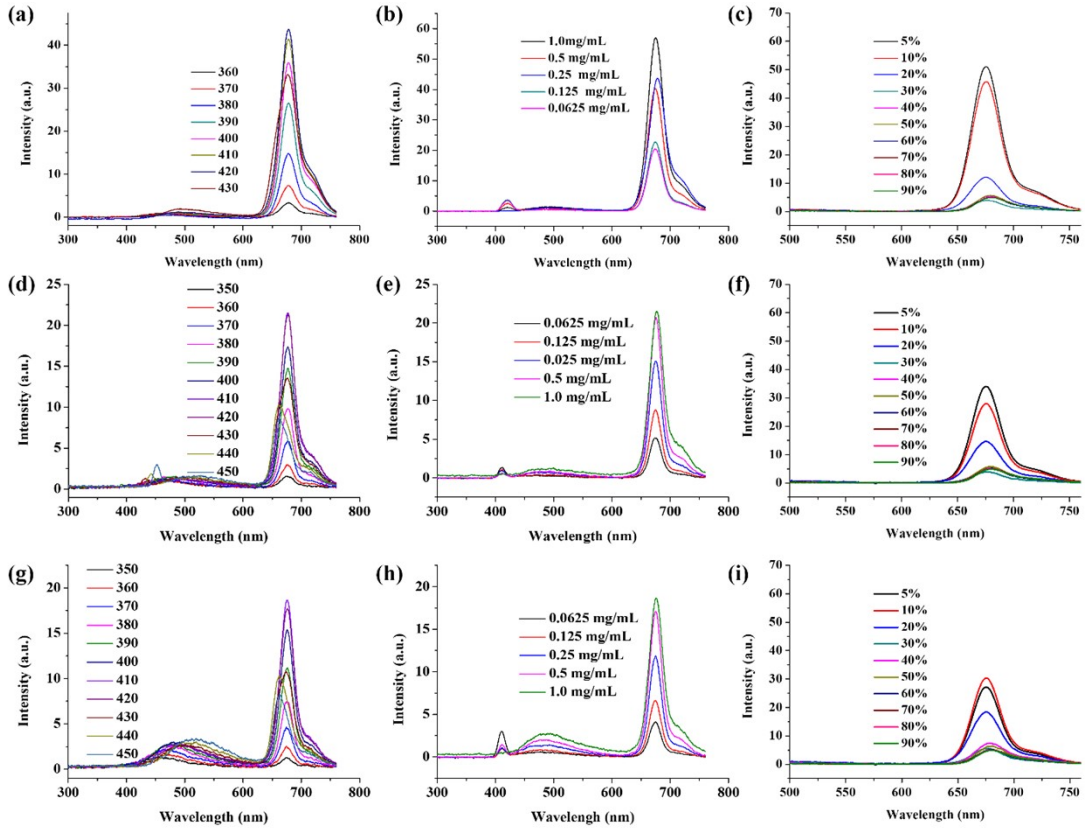


**Fig. S7** Fluorescence emission spectrum of RCQDs-120 (a-c), RCPDs-150 (d-f) and RCPDs-180 (g-i) at different excitation wavelength, concentration, and water content.

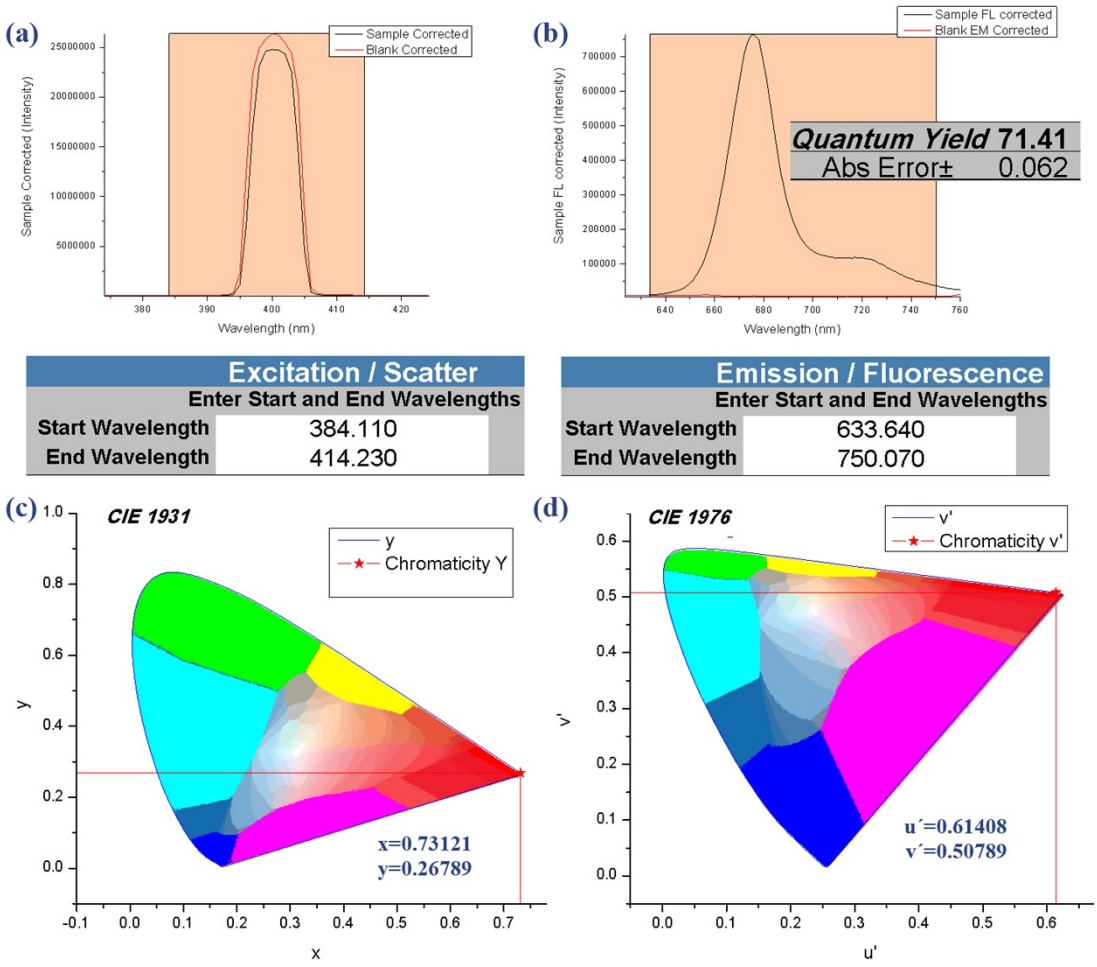


**Fig. S8** The absolute PLQY of RCPDs-120 in DMSO solution under the excitation and emission wavelength of (a) 414 nm and (b) 680 nm, the Chromatic CIE coordinates of RCPDs with CIE 1931 (c) and CIE 1976 (d).

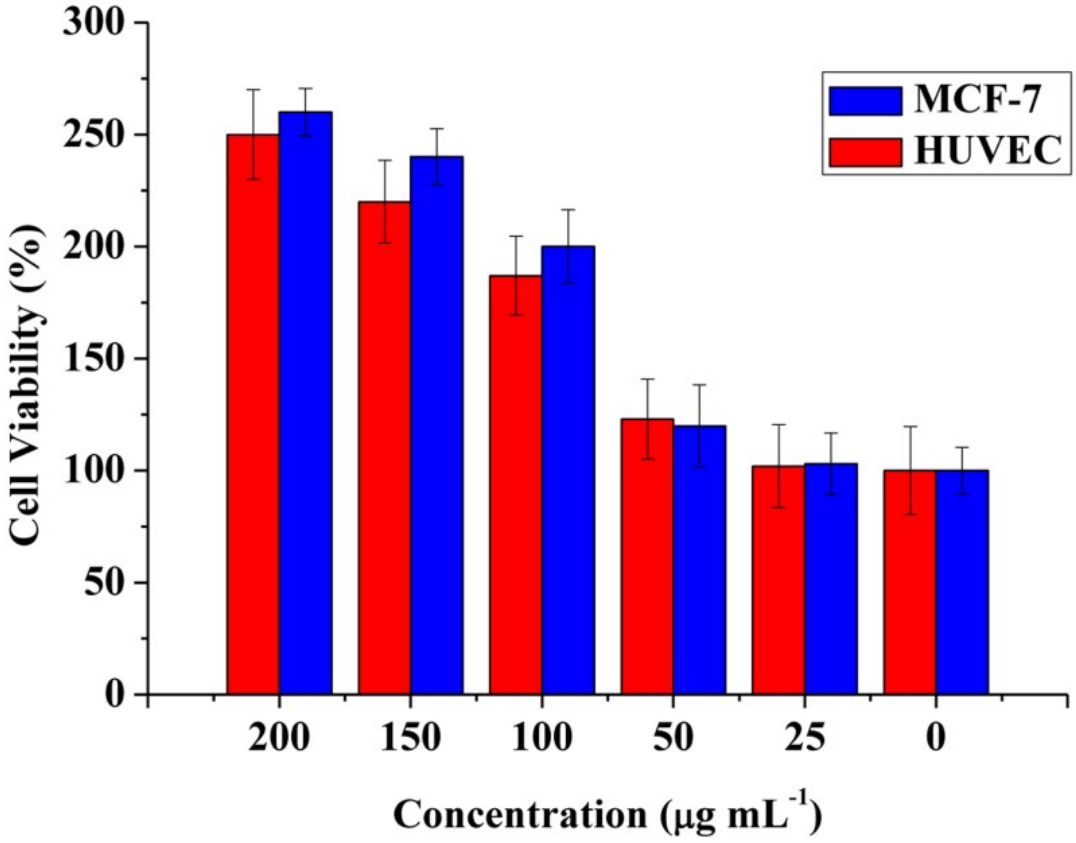


**Fig. S9** Cell viability HUVEC cells and MCF-7 cells after incubation with various concentrations of RCPDs for 24 h, respectively.

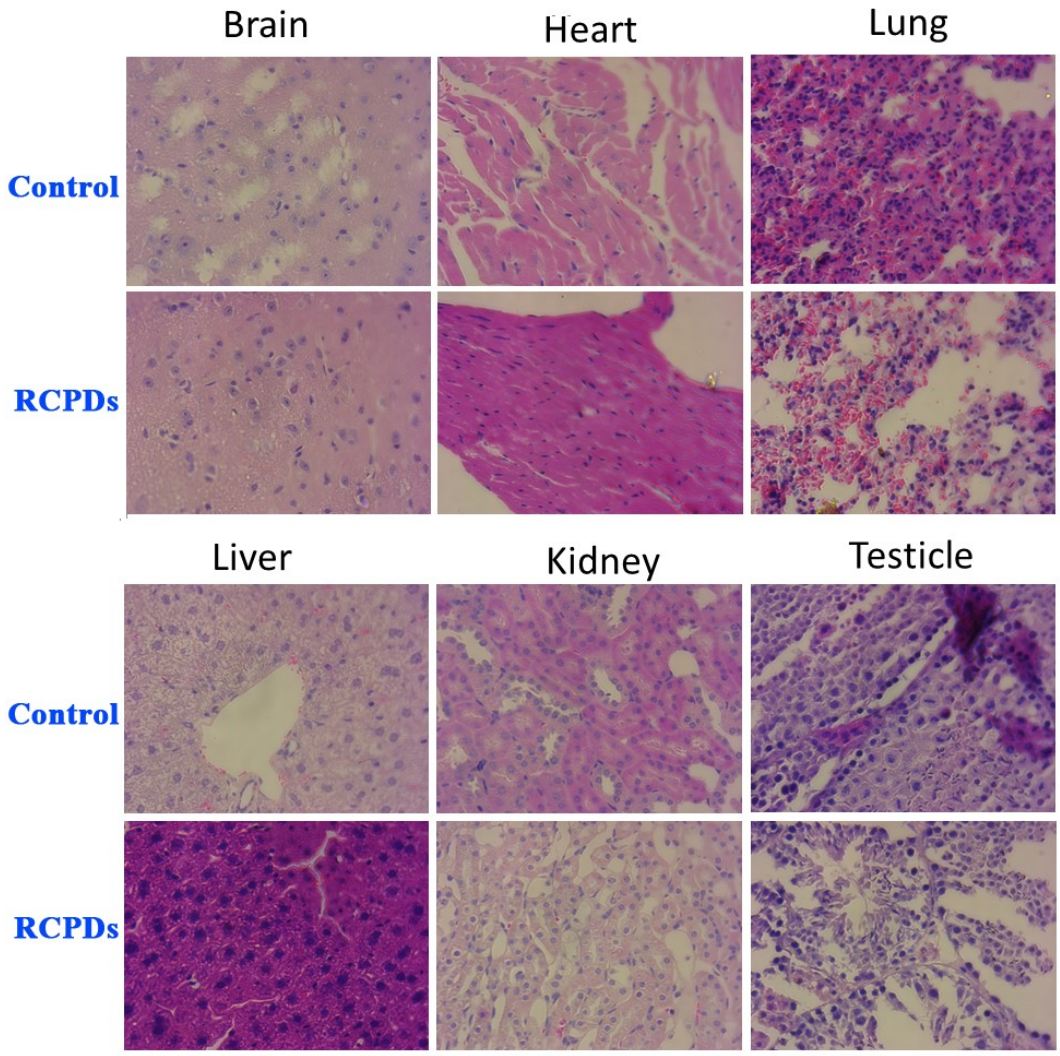


**Fig. S10** Histological evaluation of RCPDs toxicity *in vivo*. Brain, heart, lung, liver, spleen, kidney and testicle were collected from the control untreated mice and CPDs-treated mice at 7 d via intravenous injection. No symptoms of inflammation and/or lesion were observed in the images. All scale bars were 50 μm.

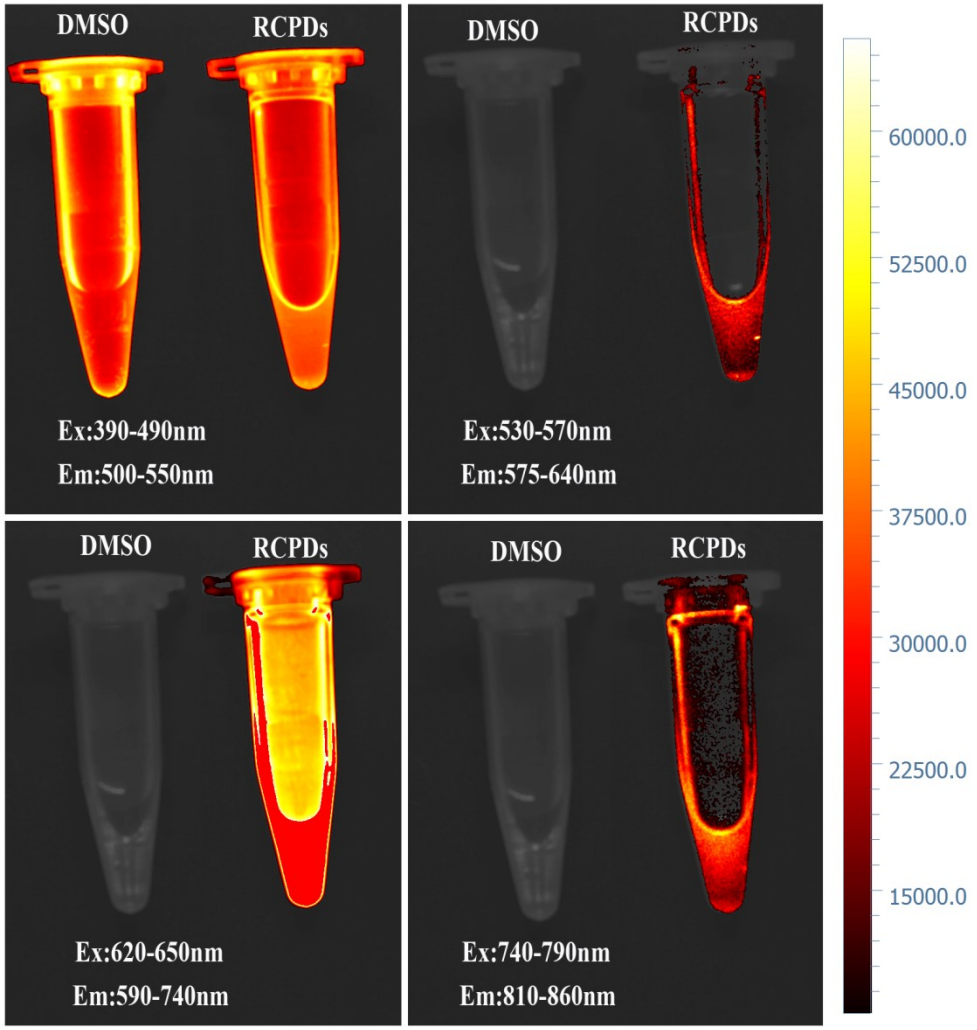


**Fig. S11** Tube fluorescence images of RCPDs-120 with 10 μg $mL^{-1}$ at various excitation wavelength

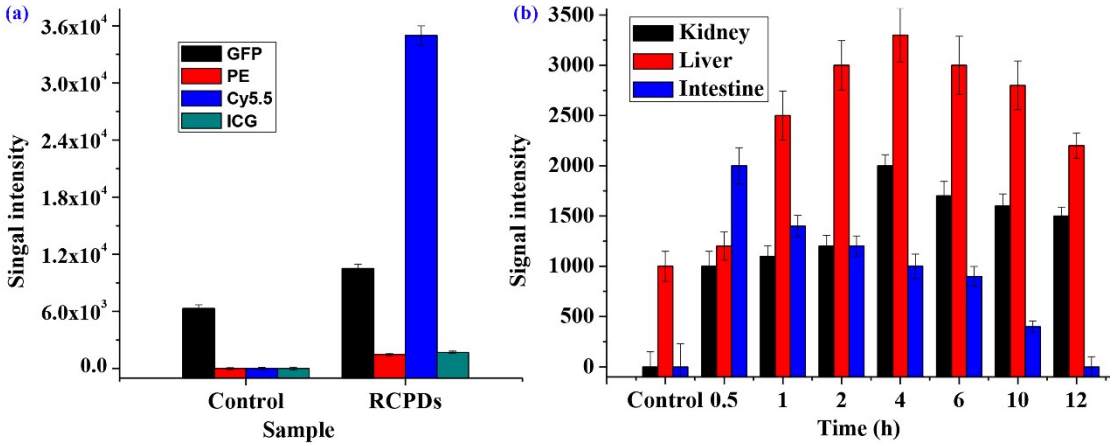


**Fig. S12** the signal intensity in the tube (a) and in liver, kidney and intestine in mice at different time points (b).

**Table S1** The relative content of chemical bonds in XPS spectra and quantum yield of RCPDs

| | C-C | C=C | C-H | C-O | COOH | C=O | QY |
|---|---|---|---|---|---|---|---|
| RCPDs-120 | 21.91% | 13.73% | 15.97% | 19.96% | 18.24% | 10.19% | 74.14% |
| RCPDs-150 | 24.36% | 30.23% | - | 12.38% | 16.35% | 16.68% | 28.25% |
| RCPDs-180 | 26.55% | 38.68% | - | 13.56% | - | 19.21% | 12.93% |